

Supporting Information

**A New Healable Polymer Material based on Ultrafast Diels-Alder ‘Click’ Chemistry using  
Triazolinedione and Fluorescent Anthracyl Derivatives; A Mechanistic Approach**

Prantik Mondal <sup>a</sup>, Gourhari Jana <sup>b</sup>, Prasanta Kumar Behera <sup>a</sup>, Pratim Kumar Chattaraj <sup>b,c</sup> and Nikhil  
K. Singha <sup>a</sup>

*<sup>a</sup> Rubber Technology Centre, Indian Institute of Technology Kharagpur, West Bengal-721302,  
India*

*<sup>b</sup> Department of Chemistry, Indian Institute of Technology Kharagpur, West Bengal-721302,  
India*

*<sup>c</sup> Department of Chemistry, Indian Institute of Technology Bombay, Powai, Mumbai-400076,  
India*

## **Contents of Supporting Information:**

<b>1. Materials.....</b>	<b>Page 3</b>
<b>2. Characterization Techniques.....</b>	<b>Page 3-5</b>
<b>3. Computational Details.....</b>	<b>Page 5</b>
<b>4. Experimental Section.....</b>	<b>Page 5-8</b>
<b>Table S1.....</b>	<b>Page 9</b>
<b>Table S2.....</b>	<b>Page10</b>
<b>Figure S1.....</b>	<b>Page 11</b>
<b>Figure S2.....</b>	<b>Page 12</b>
<b>Figure S3.....</b>	<b>Page13</b>
<b>Figure S4.....</b>	<b>Page 14</b>
<b>Figure S5.....</b>	<b>Page15</b>
<b>Figure S6.....</b>	<b>Page 16</b>
<b>Figure S7.....</b>	<b>Page 17</b>
<b>Figure S8.....</b>	<b>Page 18</b>
<b>Figure S9.....</b>	<b>Page 19</b>
<b>Figure S10.....</b>	<b>Page 20</b>
<b>Scheme S1.....</b>	<b>Page 21</b>
<b>Table S3.....</b>	<b>Page 22</b>
<b>Figure S11.....</b>	<b>Page 23</b>
<b>Figure S12.....</b>	<b>Page 24</b>
<b>Figure S13.....</b>	<b>Page 25</b>
<b>Figure S14.....</b>	<b>Page 26</b>
<b>Figure S15.....</b>	<b>Page 27</b>
<b>Figure S16.....</b>	<b>Page 28</b>
<b>Table S4.....</b>	<b>Page 29</b>
<b>Figure S17.....</b>	<b>Page 30</b>
<b>Figure S18.....</b>	<b>Page 31</b>
<b>Figure S19.....</b>	<b>Page 32</b>
<b>5. References.....</b>	<b>Page33-34</b>

## 1. Materials

Methyl methacrylate (MMA, 99%) and 2-Hydroxyethyl methacrylate (HEMA, 97 %) were purchased from Aldrich and further purified by passing through a basic alumina column to make it inhibitor-free. 9-Anthracene methanol (9-AM), Phenyl-1,2,4-triazoline-3,5-dione (PhTAD), 4-cyano-4-[(dodecylsulfanylthiocarbonyl)sulfanyl]pentanoic acid (CDTSPA), 4,4'-azobis(4-cyanovaleric acid) (ABCVA), 4,4'-Methylenebis(phenyl isocyanate), 4-(Dimethylamino)pyridine (DMAP) and 1,4-Diazabicyclo[2.2.2]octane (DABCO) were obtained from Aldrich and used as received. Bromine (>99 %) was purchased from S. D. Fine Chemical Ltd. Ethyl carbazate was purchased from Alfa Aesar and used as received. N, N'-Dicyclohexylcarbodiimide (DCC) was purchased from Spectrochem and used as received. 9-Anthracenecarboxylic acid (ACA) was obtained from Alfa-Aesar and used as received. DMF (> 99 %), THF (> 99 %) and n-Hexane (> 99 %) were purchased from Merck and used as received.

## 2. Characterization techniques

### 2.1 Gel permeation chromatography (GPC)

Gel permeation chromatography (GPC) measurement was performed at ambient temperature on Viscotek GPC instrument (model VE 3580), equipped with refractive index indicator. Tetrahydrofuran (THF) was used as an eluent with a flow rate of 1 ml/min. The system was calibrated using linear poly(methyl methacrylate) (PMMA) of narrow polydispersity index as an internal standard.

### 2.2 <sup>1</sup>H NMR and FT-IR spectroscopy

<sup>1</sup>H NMR spectra were recorded in Bruker 600 MHz spectrometer at room temperature using DMSO-d<sub>6</sub> solvent. Fourier Transform Infrared spectroscopy (FT-IR) was recorded using Perkin-

Elmer, Inc. version 5.0.1, in attenuated total reflection (ATR) mode. All the IR spectra were recorded within the range of 4000 – 400  $\text{cm}^{-1}$ .

### **2.3 Differential Scanning Calorimetry (DSC)**

Differential Scanning Calorimetry (DSC) analysis of the polymer samples was carried out using DSC 200 F3 instrument (Netzsch, Germany). All the polymer samples (~6 mg) were heated from -25  $^{\circ}\text{C}$  to +180  $^{\circ}\text{C}$  at a heating rate of 10  $^{\circ}\text{C}$  / min under  $\text{N}_2$  atmosphere. Nitrogen was used as an inert atmosphere with a flow rate of 50  $\text{mL min}^{-1}$ . The temperature against heat flow was recorded. The enthalpy was calibrated by indium standard supplied by Netzsch.

### **2.4 Nanoindentation analysis (NINT)**

The hardness value of the polymeric materials was determined by depth sensing indentation (DSI) using a TriboIndenter TI 950 (Hysitron Inc., Minneapolis, MN, USA) equipped with a diamond indenter tip of 150 nm radius. The polymer films were prepared via drop casting method (50  $\text{mg.mL}^{-1}$ ) and dried under air. The measurements were conducted at ambient temperature, and all measurements were done in a single automated run. All measurements were carried out at a fixed load of 50  $\mu\text{N}$ . The data of an average of at least ten measurements were reported in each case.

### **2.5 Optical Microscopy**

The self-healing characteristics of the polymers were studied by optical microscopy analysis. Polymer films were prepared on glass surface via drop casting method (50  $\text{mg.mL}^{-1}$ ). A notch was made on the surface of the polymer using a fine needle, and the healing of the cut surface was monitored at a different time interval.

### **2.6 Scanning Electron Microscopy (SEM) analysis**

For further verification, the healing study of the resultant polymer (50 mg.mL<sup>-1</sup>) was also studied via ZEISS EVO 60 scanning electron microscope (SEM). The polymer samples were prepared by drop-casting the solution onto a glass slide.

## 2.7 3D Optical Microscope analysis

The healing efficiency of DA polymer (50 mg.mL<sup>-1</sup>) was investigated using optical surface profilometer (OSP) by Contour GT 3D Optical Microscope, Bruker in vertical scan interferometry (VSI) mode. The polymer samples were prepared by drop-casting the solution onto a glass slide.

$$\text{Healing efficiency (HE) (\%)} = \left[ \frac{(d_{\text{healed}} - d_{\text{damaged}})}{(d_{\text{undamaged}} - d_{\text{damaged}})} \right] \times 100$$

Here,  $d_{\text{undamaged}}$ ,  $d_{\text{damaged}}$ , and  $d_{\text{healed}}$  indicate the surface profile depth before scratch, after scratch, and for final healable surface.

$$d_{\text{undamaged}} = 0.0 \text{ }\mu\text{m (undamaged smooth polymer surface, before scratch)}$$

$$d_{\text{damaged}} = 14 \text{ }\mu\text{m (notch depth after scratch)}$$

$$d_{\text{healed}} = 3 \text{ }\mu\text{m (notch depth after heal)}$$

$$\text{HE (\%)} = \left[ \frac{(3-14)}{(0-14)} \right] \times 100 = \sim 80 \%$$

## 2.8 UV-Vis Spectroscopy

UV-Vis spectroscopy analysis of the organic compounds (20 mg.mL<sup>-1</sup>) and polymer samples (50 mg.mL<sup>-1</sup>) were carried out in Perkin-Elmer UV/Vis Spectroscopy Lambda 35, using DMF or THF as solvent.

## 3. Computational Details

All of the structures optimization included in this study followed by frequency calculations were performed using a long-range dispersion corrected functional based on the meta-GGA

approximation M06-2X<sup>1,2</sup> with the 6-311+G(d, p)<sup>3,4</sup> basis set in presence of a solvent. The transition state search and subsequent intrinsic reaction coordination (IRC) calculations were carried out to authenticate that the located transition states (TSs) corresponds to the correct stationary points. Solvent effects were modelled by adopting a polarizable continuum model (PCM).<sup>5-7</sup> The GAUSSIAN 09 software package<sup>8</sup> was used for all the calculations. The thermochemical and kinetic parameters like Gibbs free energy changes ( $\Delta G$ ), kinetic free energy barriers ( $\Delta G^\ddagger$ ) were computed and the corresponding rate constants were obtained to study the reaction mechanism using the most widely used global hybrid meta-GGA functional M06-2X with 54% HF exchange as the candidate of Minnesota functional family. It is one of the well-balanced functionals for overall good performance across the broad areas of chemistry including thermochemistry and reaction kinetics, but excluding the multi-reference systems such as those containing transition metals. There are a series of studies where this functional performs better over other popular DFT functionals for applications involving main group thermochemistry, organometallic chemistry, noncovalent interactions, kinetics, and electronic excitation energies.<sup>9-</sup>

<sup>16</sup>

## 4. Experimental Section

### 4.1 Preparation of PHEMA-*co*-PMMA (P1) via RAFT polymerization:

The copolymerization of HEMA and MMA monomers were carried out using CDTSPA as a chain transfer agent (CTA) and ABCVA as a thermal initiator. In this copolymerization reaction, MMA (1 g,  $9.9 \times 10^{-3}$  mol), HEMA (3.89 g,  $2.9 \times 10^{-2}$  mol), CDTSPA (0.16 g,  $3.99 \times 10^{-4}$  mol) and ABCVA (0.028 g,  $9.9 \times 10^{-5}$  mol) were dissolved in DMF (4 ml) taken in a Schlenk tube. The system was sealed by a silicon septum and made free of oxygen by purging nitrogen

throughout the mixture for 15-20 mins with continuous stirring. The tube was then placed in an oil bath preset at 80 °C and allowed to continue the reaction for 16 h. After the reaction was terminated, the tube was immediately placed in an ice bath and exposed to air. Later the polymer was dissolved in a little volume of DMF followed by precipitating several times in cold diethyl ether. The material was then dried in vacuum for several characterizations. ( $M_{n, \text{NMR}} = 9300 \text{ g mol}^{-1}$ ,  $M_{n, \text{Theo.}} = 9000 \text{ g mol}^{-1}$ ).

#### **4.2 Functionalization of the P1 copolymer with anthracyl groups:**

The typical modification of the pendant hydroxyl groups of the P1 copolymer was carried out using ACA via DCC and DMAP coupling reaction. In a 100 ml round bottomed flask the reaction mixture containing (0.83 g,  $4.0 \times 10^{-3} \text{ mol}$ ) DCC, (0.049 g,  $4.0 \times 10^{-4} \text{ mol}$ ) DMAP and (0.89 g,  $4.0 \times 10^{-3} \text{ mol}$ ) ACA in 1.5 ml DMF was allowed to rotate at 0 °C for ~15 mins. Meanwhile, the copolymer (0.5 g,  $5.4 \times 10^{-5} \text{ mol}$ ) was dissolved in 0.5 ml of DMF and added dropwise to the above mixture at the mentioned temperature. The reaction was further allowed to continue for an hour at 0 °C followed by gentle warming to the room temperature, and then the reaction was further carried out for 24 h. the final product of the reaction mixture was filtered and precipitated in excess cold diethyl ether followed by repeated washing to obtain the fine canary yellow colour anthracyl modified copolymer. The resultant copolymer was dried in vacuum oven for further analyses such as FT-IR,  $^1\text{H}$  NMR, GPC and DSC analyses.

#### **4.3 Preparation of bifunctional TAD derivative:**

The preparation of bifunctional TAD derivative has been prepared following the procedures mentioned in literatures.<sup>17,18</sup>

#### **4.4 Preparation of thermoreversible P1-Anthracene-bisTAD crosslinked DA network:**

The ultrafast synthesis of the crosslinked network via conventional Diels-Alder reaction was carried out at room temperature within few seconds. The details of the reaction procedure are as follows. The copolymer (0.1 g,  $6.5 \times 10^{-6}$  mol) and bifunctional TAD derivative (0.002 g,  $6.5 \times 10^{-6}$  mol) were taken at an equimolar ratio and dissolved separately in THF. The TAD solution was added to the polymer solution which resulted in an ultrafast crosslinked gel. However, for completion, the reaction was further continued for 2 mins at room temperature (as evidenced by the gradual disappearance of the red colour of the azo derivative). The resultant network was dried in vacuum oven for further detailed analyses.

#### **4.5 DA Reaction of 9-Anthracene methanol (9-AM) and PhTAD**

As an analogous to polymer-bisTAD reaction system, 9-AM (0.050 g,  $2.25 \times 10^{-4}$  mol, 0.4 mL DMF) and PhTAD (0.035 g,  $2.04 \times 10^{-4}$  mol, 0.4 mL DMF) were taken separately at 1: 0.90 molar ratio in DMF solvent. The former solution was added to later under ambient conditions. As soon as the 9-AM solution was added to the TAD solution, the red colour of the later one gradually disappears. It took almost 3 min for completion of the overall reaction as observed from the complete discolouration of the azo derivative. The final product was kept for further analyzing.

#### **4.6 DA reaction of Anthracyl modified copolymer and PhTAD**

The P1 copolymer (0.05 g,  $3.26 \times 10^{-6}$  mol) and PhTAD (0.003 g,  $1.63 \times 10^{-5}$  mol) were taken separately at 1:5 molar ratio and dissolved in THF. Later on, the TAD solution was added to the polymer solution at room temperature. The reaction was allowed to continue until the disappearance of the red colour of the azo derivative. The final reaction mixture was kept for further spectroscopic analyses.



**Table S1:**Summary of copolymers of HEMA and MMA at different feed ratios prepared via RAFT polymerization using CDTSPA as RAFT agent and ABCVA as thermal initiator.

<b>Sample Code</b>	<b>Monomer Feed Ratio HEMA (M<sub>1</sub>): MMA(M<sub>2</sub>)<sup>a</sup></b>	<b>Total Monomer Conversion (%)</b>	<b>M<sub>n</sub>, Theo</b>	<b>M<sub>n</sub>, NMR<sup>b</sup></b>	<b>Copolymer composition HEMA (m<sub>1</sub>) : MMA (m<sub>2</sub>) (mol %)<sup>c</sup></b>
P1	75:25	75	9000	9800	77:23
P2	50:50	55	6000	4600	51:49
P3	25:75	40	3000	3500	29:71

<sup>a</sup> The molar ratio of HEMA and MMA monomers used is [monomer]:[RAFT]:[initiator] = 100:1:0.25.

<sup>b</sup> M<sub>n</sub>, NMR has been calculated from determining the ratio of integrated peak areas of -OCH<sub>2</sub> protons of PHEMA unit and -OCH<sub>3</sub> protons of PMMA unit to -SCH<sub>2</sub> protons of RAFT end group.

<sup>c</sup> Copolymer composition was determined from <sup>1</sup>H NMR analysis.

**Table S2:** Summary of anthracene modified copolymers

<b>Sample Code</b>	<b><math>M_{n, GPC} (g\ mol^{-1})^a</math></b>	<b><math>M_{n, NMR} (g\ mol^{-1})^b</math></b>	<b>PDI<sup>a</sup></b>
P1-Anthracene copolymer	15300	13300	1.6
P2- Anthracene copolymer	11500	9000	1.5
P3- Anthracene copolymer	7000	6900	1.2

<sup>a</sup>  $M_{n, GPC}$  has been calculated using THF as an eluent.

<sup>b</sup>  $M_{n, NMR}$  has been calculated from determining the ratio of integrated peak areas of -OCH<sub>2</sub> protons of PHEMA unit and -OCH<sub>3</sub> protons of PMMA unit to -SCH<sub>2</sub> protons of RAFT end group.

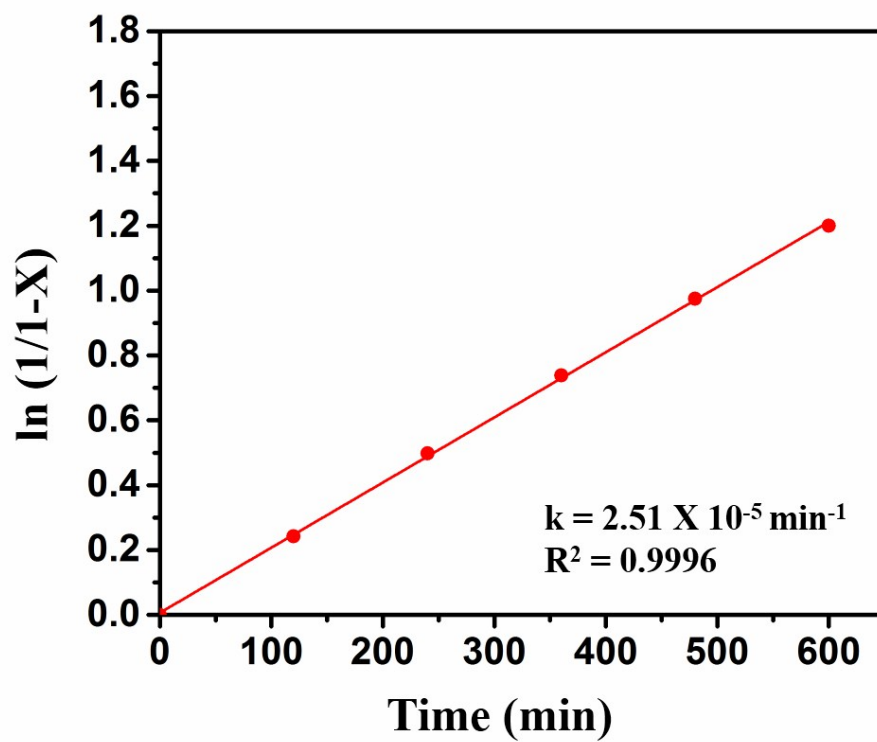


**Fig S1:** Kinetic analysis of P1 copolymer prepared via RAFT polymerization using CDTSPA as RAFT agent and ABCVA as thermal initiator.

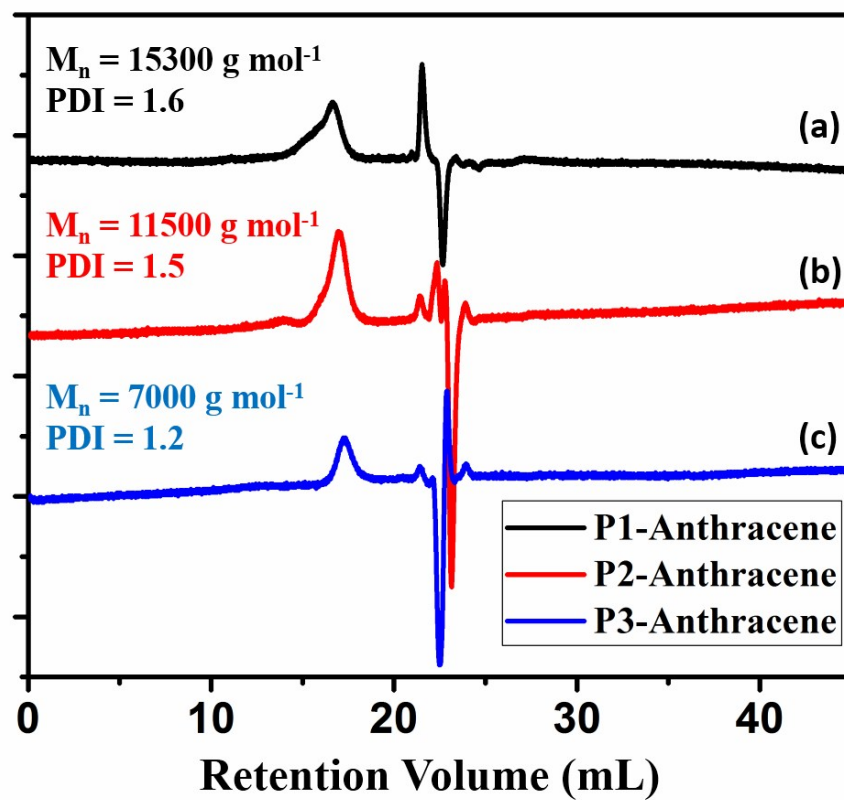


**Fig S2:** GPC elution curves of anthracyl modified copolymers using THF as an eluent, (a) P1-Anthracene copolymer, (b) P2-Anthracene copolymer and (c) P3-Anthracene copolymer.

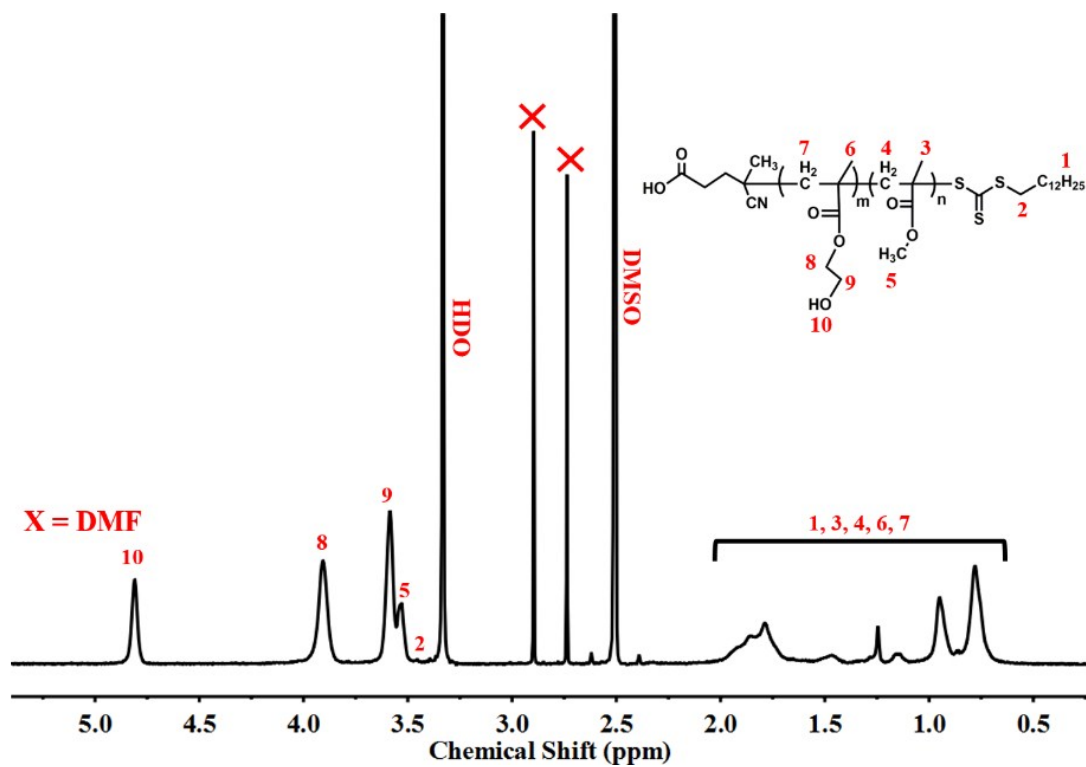


**Fig S3:**  $^1\text{H}$  NMR analysis of P1 copolymer in  $\text{DMSO-d}_6$  solvent

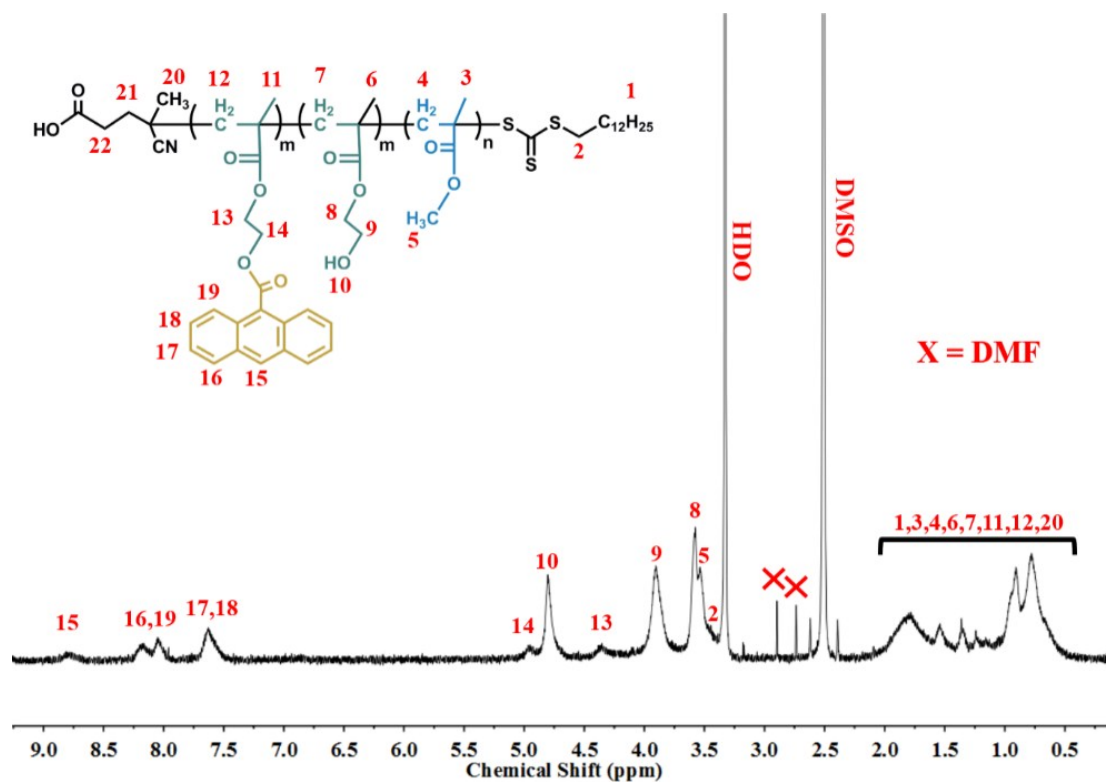
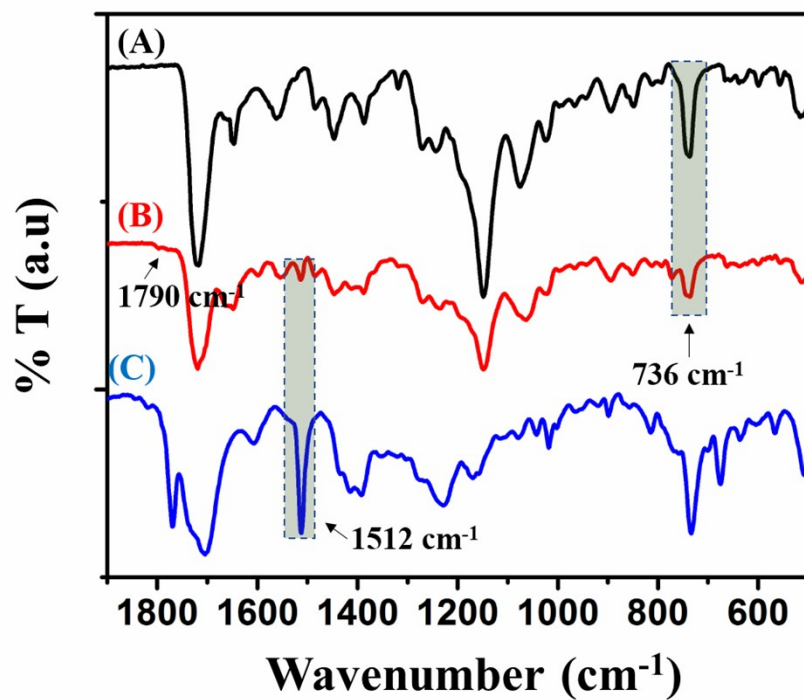


**Fig S4:**  $^1\text{H}$  NMR analysis of P1-Anthracene copolymer in  $\text{DMSO-d}_6$  solvent.



**FigureS5:** (A) P1-Anthracene copolymer; (B) P1-Anthracene-bisTAD network and (C) bisTAD.

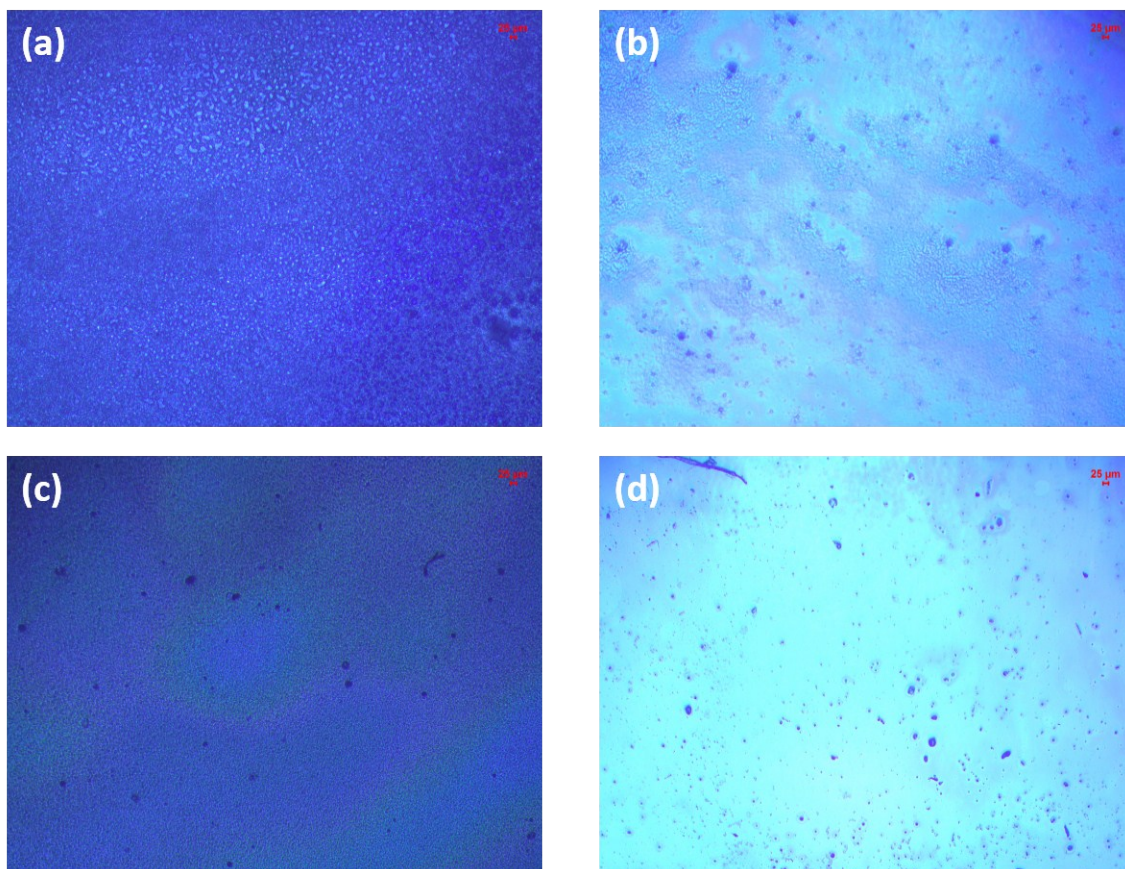


**Figure S6:** Fluorescence microscopy images of (a) P2-Anthracene copolymer film, (b) P2-Anthracene-bisTAD crosslinked copolymer film, (c) P3-Anthracene copolymer film and (d) P3-Anthracene-bisTAD crosslinked copolymer film.



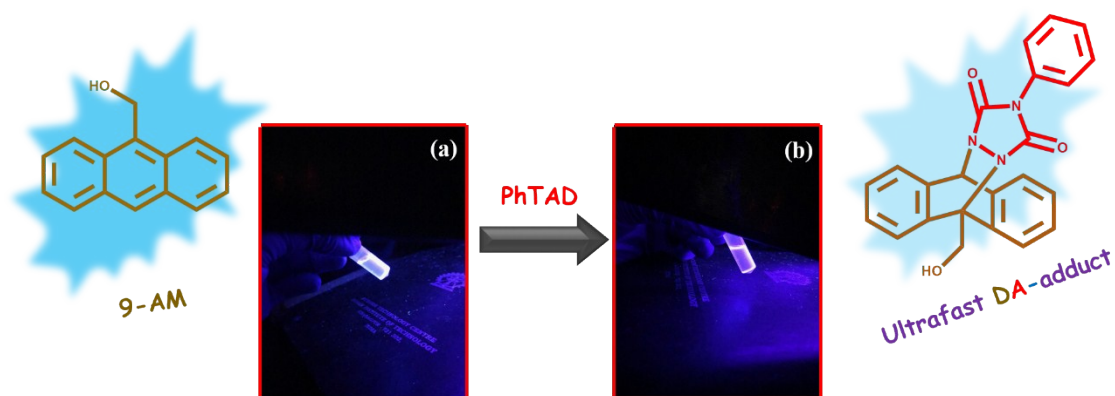


**Figure S7:** (a) 9-AM emitting bright fluorescence and (b) Quenched fluorescence of 9-AM-PhTAD DA adduct (9-AM: PhTAD = 1: 0.9 molar ratio) in DMF solvent.

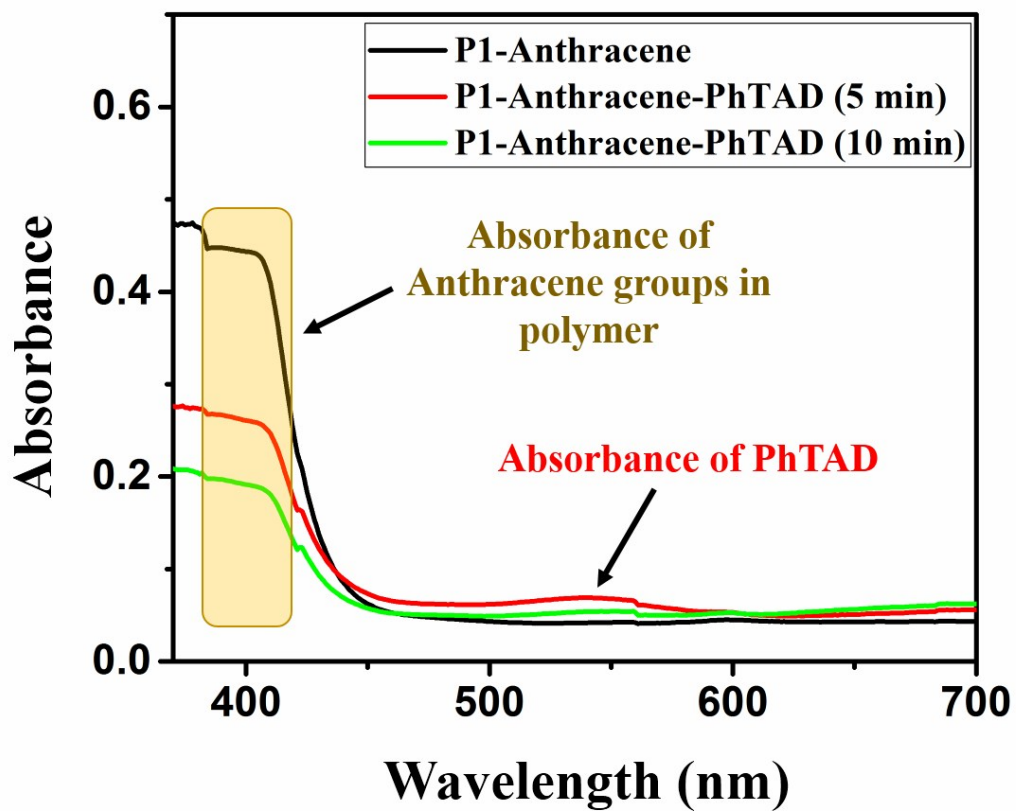


**Figure S8:** UV analysis of P1-Anthracene-PhTAD copolymer before and after the reaction completion.

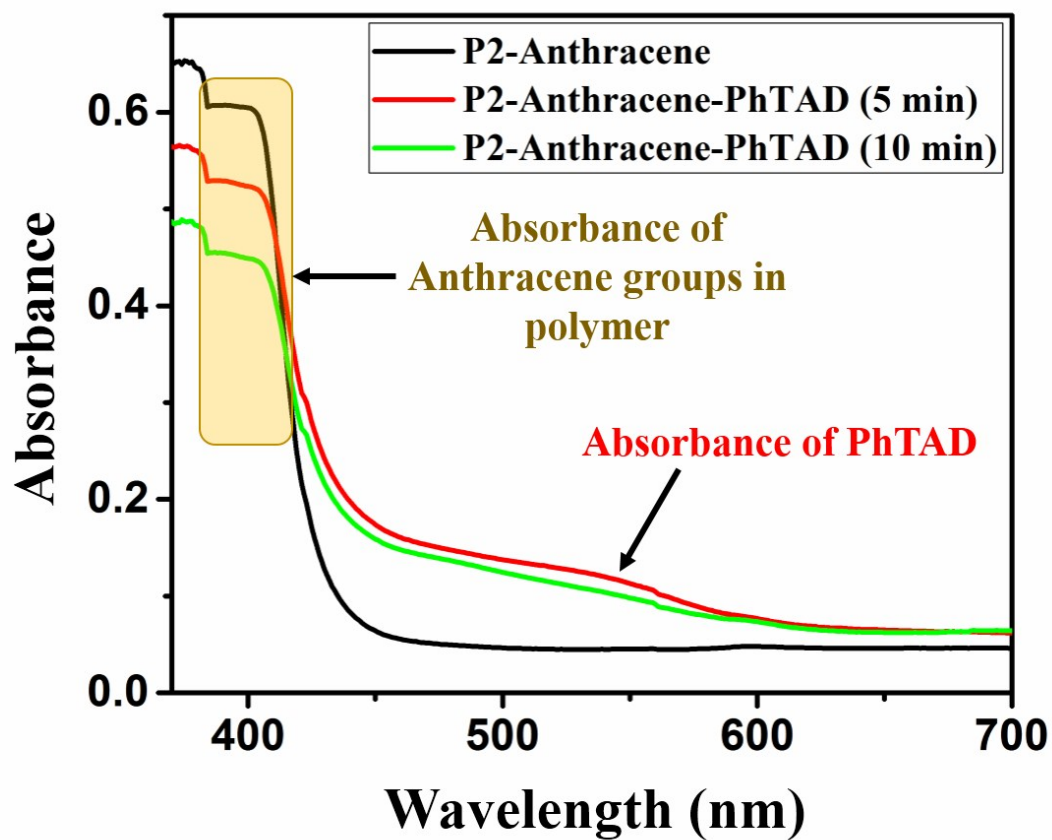


**Figure S9:** UV analysis of P2-Anthracene-PhTAD copolymer before and after the reaction completion.

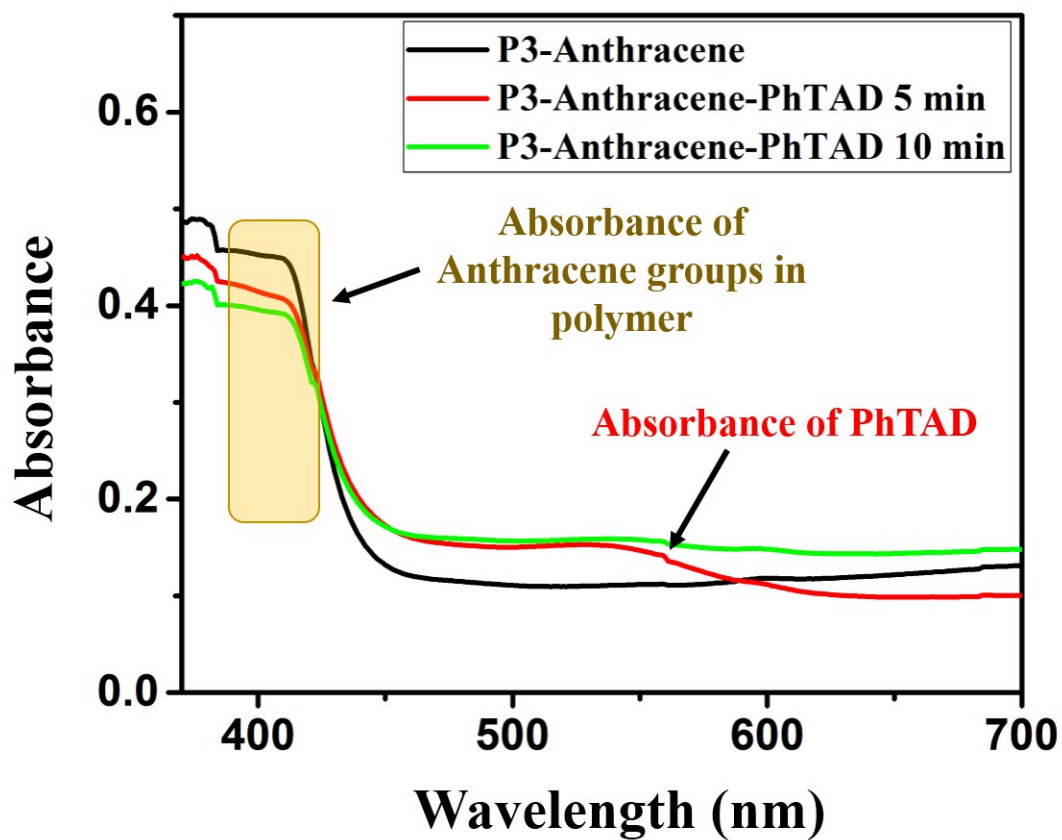
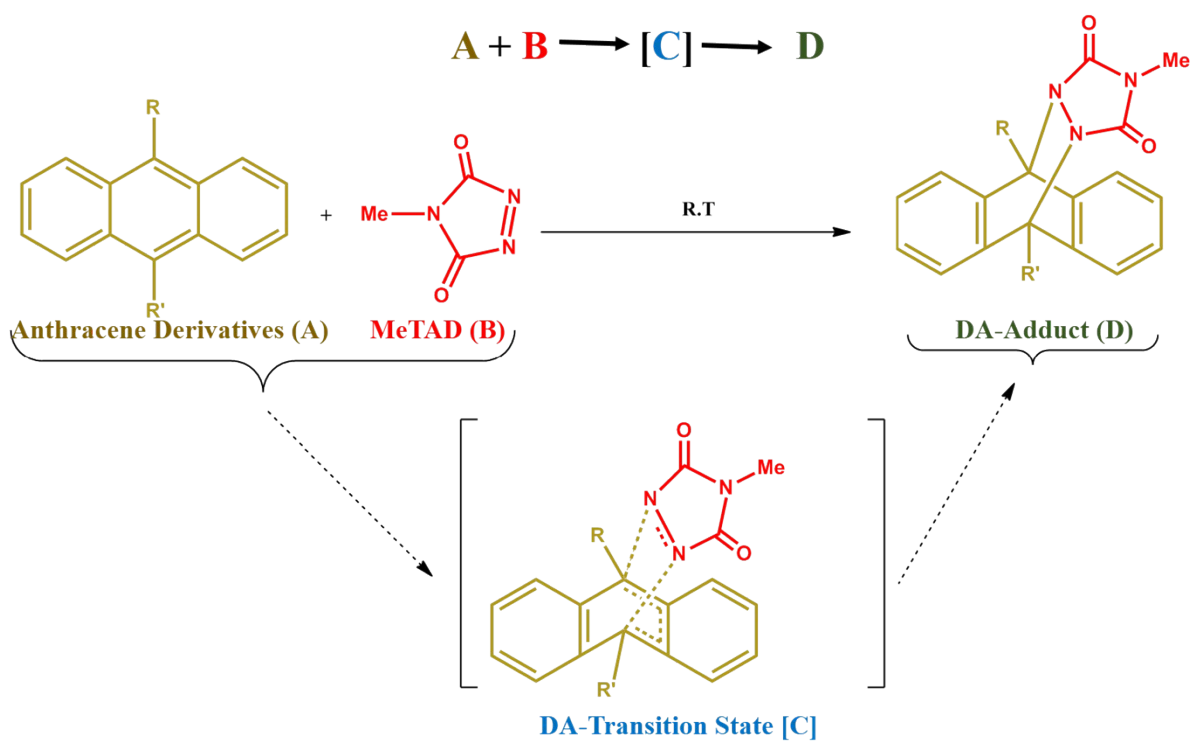


**Figure S10:** UV analysis of P3-Anthracene-PhTAD copolymer before and after the reaction completion.



**Scheme S1:** DA-reaction mechanism of Anthracene-derivatives and N-Methyl-TAD (MeTAD)

**Table-S3:** Various competitive Diels-Alder reactions studied in gas phase along with their free energy barriers ( $\Delta G^\ddagger$ ) and product stabilization free energies ( $\Delta G$ ) given in kcal/mol

<b>No.</b>	<b>-R</b>	<b>-R'</b>	<b>Free energy barrier (<math>\Delta G^\ddagger</math>) (kcal/mol)</b>	<b>Product stability (<math>\Delta G</math>) (kcal/mol)</b>	<b>Rate constant (s<sup>-1</sup>)</b>
<b>1</b>	-COOMe	-H	20.7	-15.9	0.0035
<b>2</b>	-Me	-H	14.2	-20.5	218
<b>3</b>	-COOMe	-COOMe	21.9	-16.7	0.0005
<b>4</b>	-Me	-Me	13.1	-21.7	1408
<b>5</b>	-COOMe	-Me	15.9	-21.5	12.22

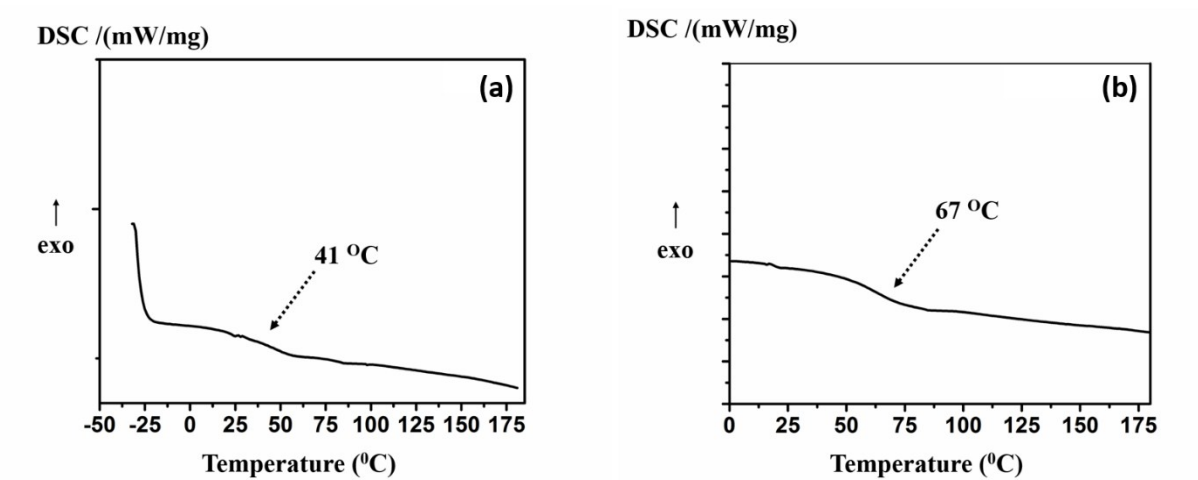


**Figure S11:** Glass transition temperature of P1-anthracene (a) and (b) P1-anthracene-bisTAD polymer.

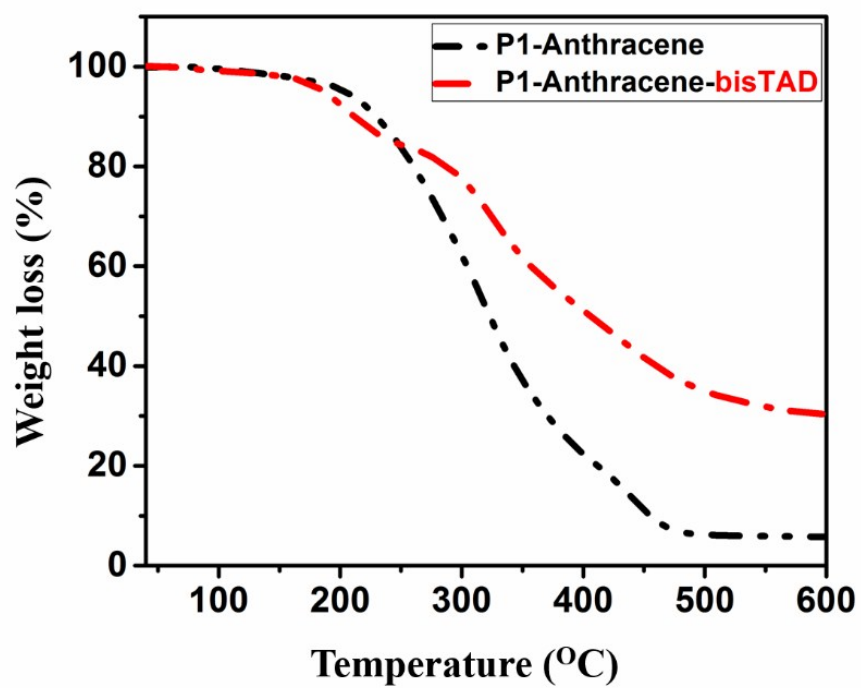


**Fig S12:** TGA analysis of P1-Anthracyl copolymer and its TAD modified DA crosslinked form.



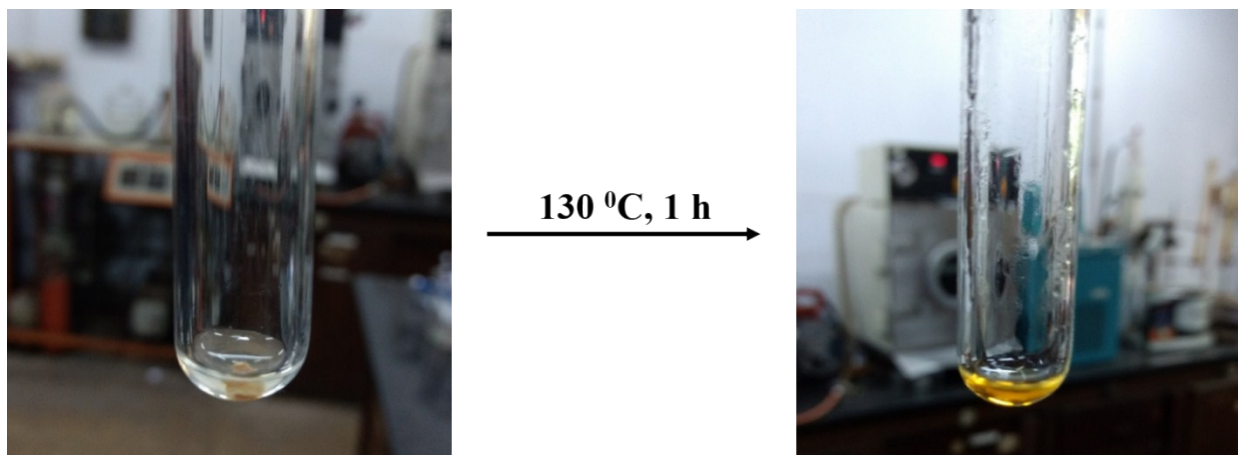


**Figure S13:** Solubility study of Anthracene modified copolymer-bisTAD adduct (a) at room temperature and (b) after heating at  $\sim 130\text{ }^{\circ}\text{C}$  for  $\sim 1\text{ h}$ .

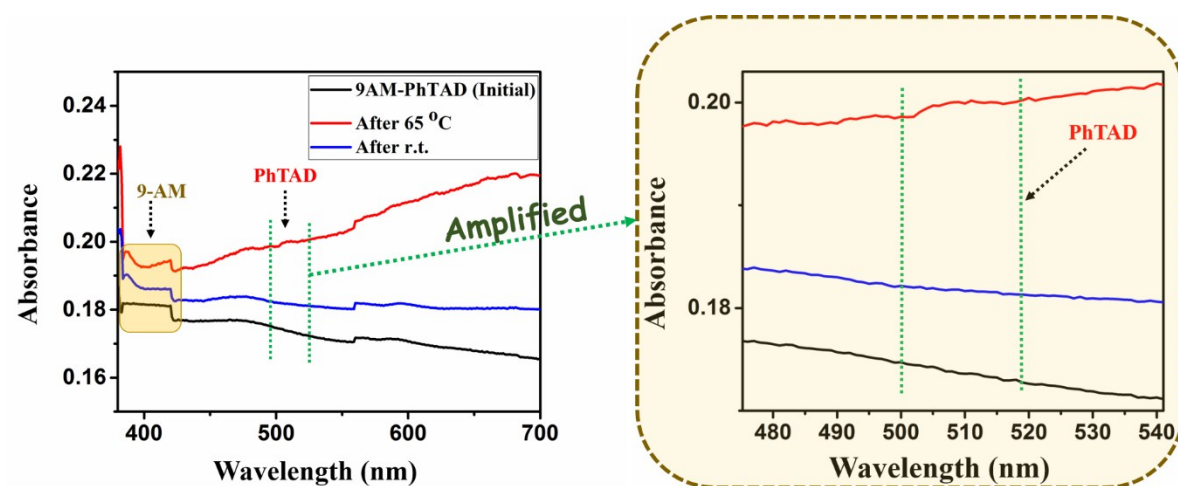


**Figure S14:** Thermoreversibility analysis of 9-AM-PhTAD DA bonds via UV-Vis spectroscopy.

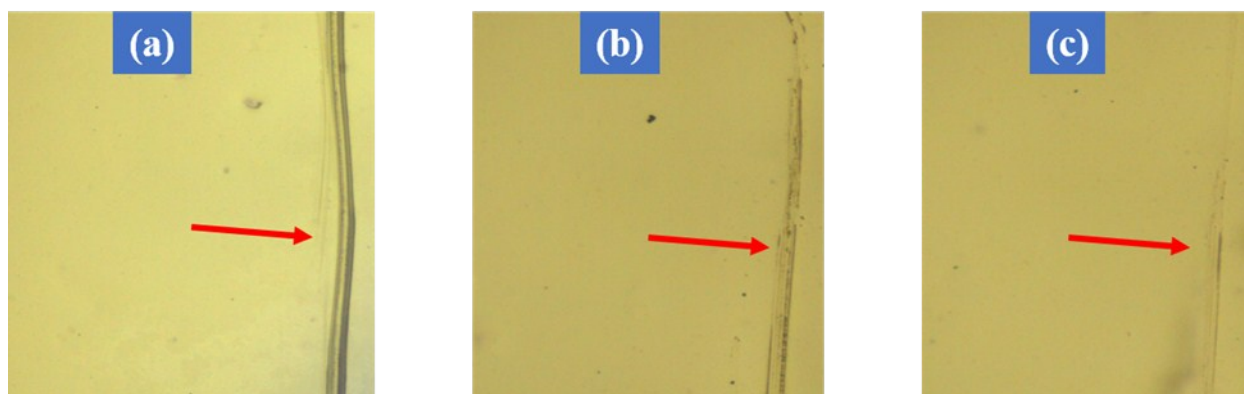


**Figure S15:** Optical microscopy images of **(A)** notched P1-Anthracene-bisTAD; **(B)** healed P1-Anthracene-bisTAD polymer surface after 3 h and **(C)** healed P1-Anthracene-bisTAD polymer surface after 5h heating at a retro-DA temperature.

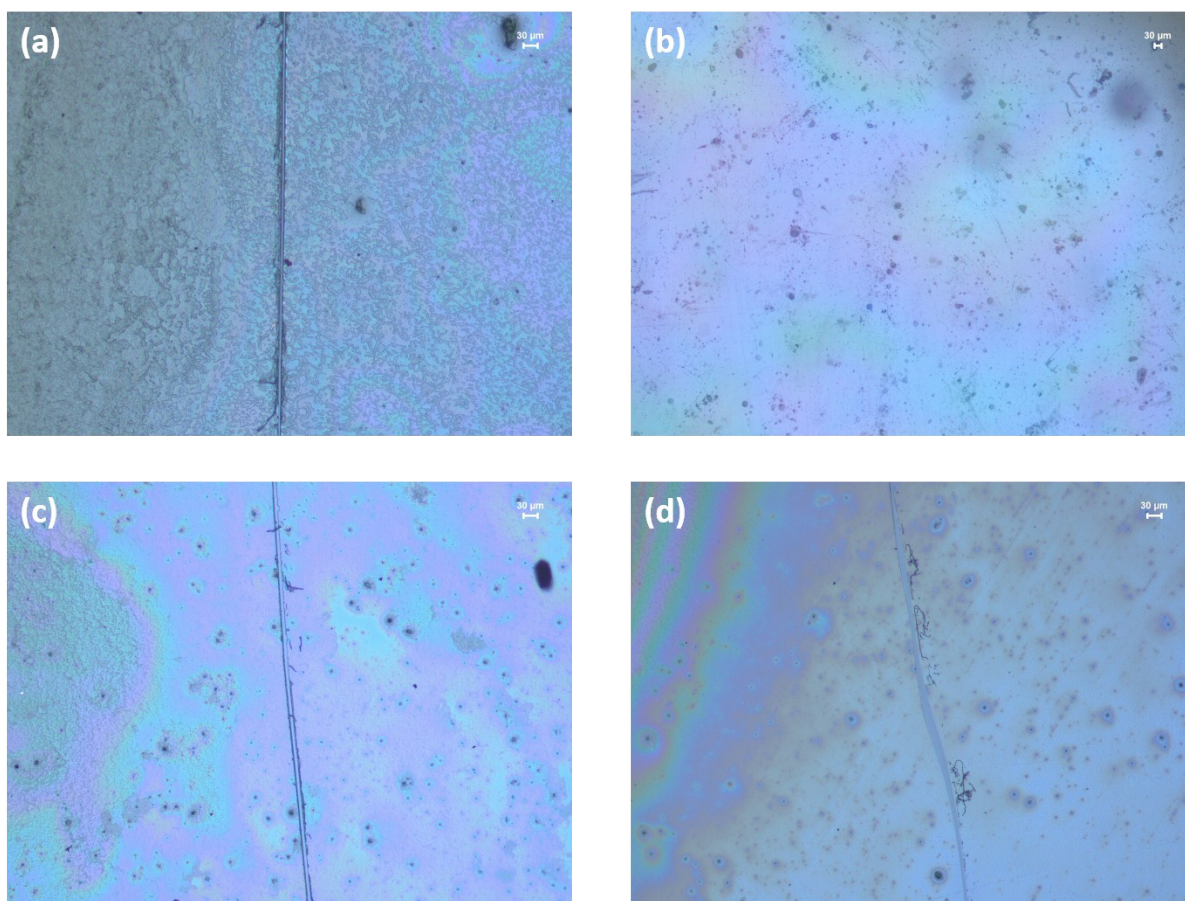


**Figure S16:** Optical microscopy images of (a) notched P2-Anthracene-bisTAD film; (b) after heating at  $\sim 130$   $^{\circ}\text{C}$  for  $\sim 5$  h followed by cooling to room temperature, (c) notched P3-Anthracene-bisTAD and (d) after heating at  $\sim 130$   $^{\circ}\text{C}$  for  $\sim 5$  h followed by cooling to room temperature.

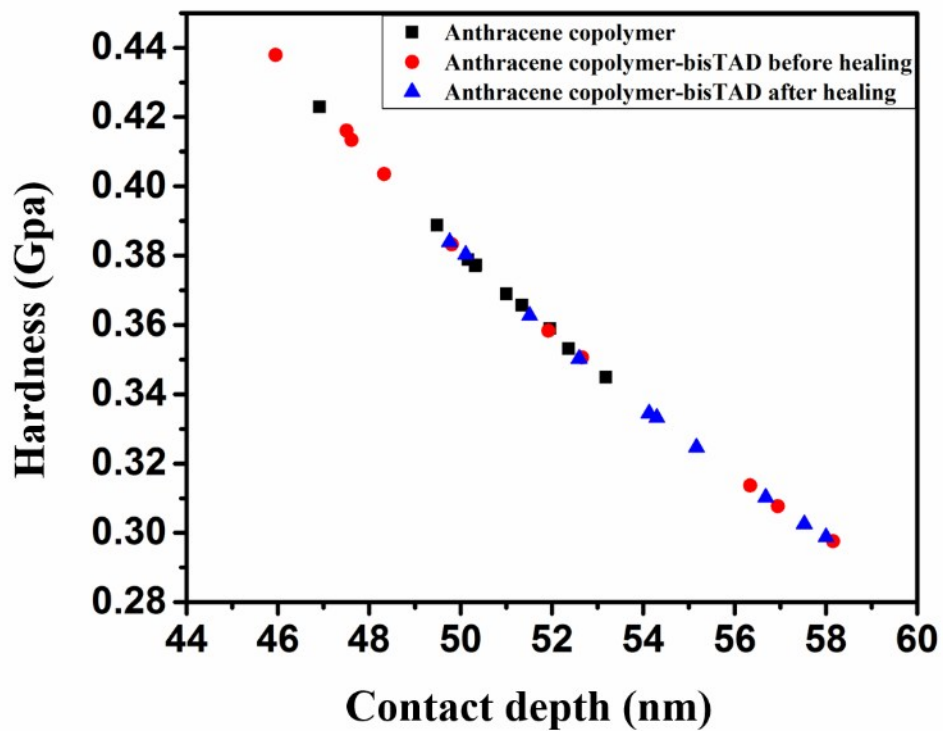


**Figure S17:** NINT analysis of (a) P1-Anthracene copolymer, (b) P1-Anthracene copolymer-bisTAD before healing and (c) P1-Anthracene copolymer-bisTAD after healing.

**Table S4:** Nanoindentation analysis of P2-Anthracene-bisTAD and P3-Anthracene-bisTAD crosslinked polymer samples before and after healing

<b>Polymer Samples</b>	<b>Contact Depth (nm)</b>	<b>Hardness (GPa)</b>
<b>P2-Anthracene-bisTAD before healing</b>	36.08	0.62
<b>P2-Anthracene-bisTAD after healing</b>	38.62	0.55
<b>P3-Anthracene-bisTAD before healing</b>	23.34	1.17
<b>P3-Anthracene-bisTAD after healing</b>	22.65	1.22

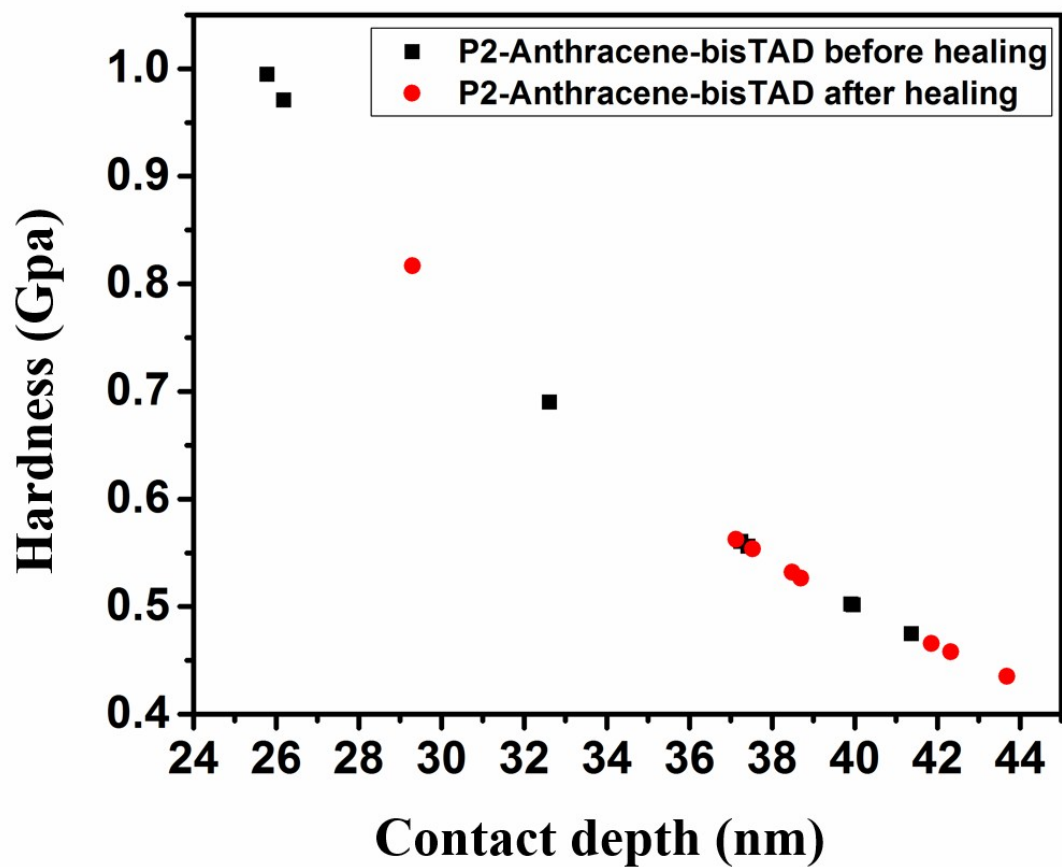


**Figure S18:** NINT analysis of (a) P2-Anthracene copolymer-bisTAD before healing and (b) P2-Anthracene copolymer-bisTAD after healing.

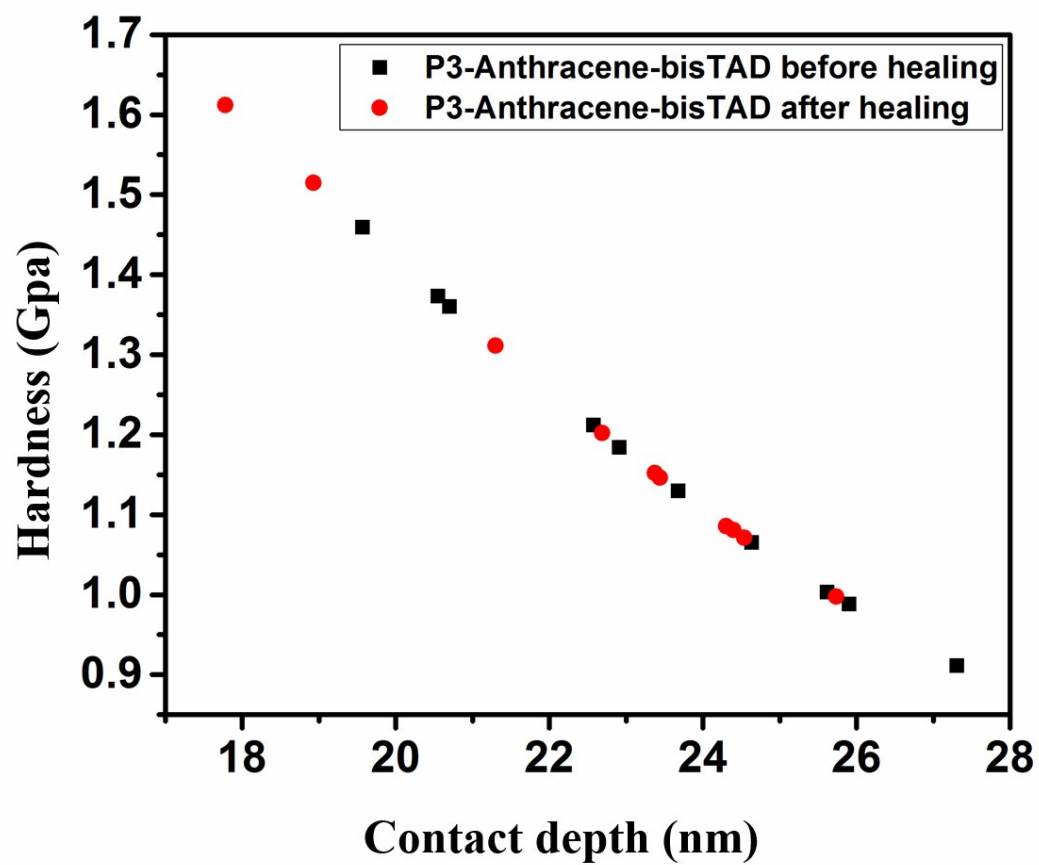


**Figure S19:** NINT analysis of(a) P3-Anthracene copolymer-bisTAD before healing and (b) P3-Anthracene copolymer-bisTAD after healing.



## 5. References:

1. Y. Zhao and D. G. Truhlar, *Theor. Chem. Acc.*, 2008, **120**, 215.
2. L. P. Liu, D. Malhotra, R. S. Paton, K. Houk and G. B. Hammond, *Angew. Chem. Int. Ed.*, 2010, **49**, 9132.
3. R. Krishnan, J. S. Binkley, R. Seeger and J. A. Pople, *J. Chem. Phys.*, 1980, **72**, 650.
4. T. Clark, J. Chandrasekhar, G. W. Spitznagel and P. V. R. Schleyer, *J. Comput. Chem.*, 1983, **4**, 294.
5. S. Miertuš, E. Scrocco and J. Tomasi, *Chem. Phys. Lett.*, 1981, **55**, 117.
6. V. Barone, M. Cossi and J. Tomasi, *J. Chem. Phys.*, 1997, **107**, 3210.
7. M. Cossi, G. Scalmani, N. Rega and V. Barone, *J. Chem. Phys.*, 2002, **117**, 43.
8. Gaussian 09, Revision D.01, M. J. Frisch, G. W. Trucks, H. B. Schlegel, G. E. Scuseria, M. A. Robb, J. R. Cheeseman, G. Scalmani, V. Barone, B. Mennucci, G. A. Petersson, H. Nakatsuji, M. Caricato, X. Li, H. P. Hratchian, A. F. Izmaylov, J. Bloino, G. Zheng, J. L. Sonnenberg, M. Hada, M. Ehara, K. Toyota, R. Fukuda, J. Hasegawa, M. Ishida, T. Nakajima, Y. Honda, O. Kitao, H. Nakai, T. Vreven, J. A. Montgomery, Jr., J. E. Peralta, F. Ogliaro, M. Bearpark, J. J. Heyd, E. Brothers, K. N. Kudin, V. N. Staroverov, T. Keith, R. Kobayashi, J. Normand, K. Raghavachari, A. Rendell, J. C. Burant, S. S. Iyengar, J. Tomasi, M. Cossi, N. Rega, J. M. Millam, M. Klene, J. E. Knox, J. B. Cross, V. Bakken, C. Adamo, J. Jaramillo, R. Gomperts, R. E. Stratmann, O. Yazyev, A. J. Austin, R. Cammi, C. Pomelli, J. W. Ochterski, R. L. Martin, K. Morokuma, V. G. Zakrzewski, G. A. Voth, P. Salvador, J. J. Dannenberg, S. Dapprich, A. D. Daniels, O.

Farkas, J. B. Foresman, J. V. Ortiz, J. Cioslowski, D. J. Fox, Gaussian, Inc., Wallingford CT, **2013**.

9. Y. Zhao and D. G. Truhlar, *Theor. Chem. Acc.*, 2008, **120**, 215-241.
10. Y. Zhao and D. G. Truhlar, *J. Phys. Chem. A*, 2006, **110**, 13126-13130.
11. Y. Zhao and D. G. Truhlar, *J. Chem. Phys.*, 2006, **125**, 194101.
12. C. A. Morgado, P. Jurečka, D. Svozil, P. Hobza and J. Šponer, *Phys. Chem. Chem. Phys.*, 2010, **12**, 3522-3534.
13. M. Walker, A. J. Harvey, A. Sen and C. E. Dessent, *J. Phys. Chem. A*, 2013, **117**, 12590-12600.
14. S. A. Smith, K. E. Hand, M. L. Love, G. Hill and D. H. Mager, *J. Comput. Chem.*, 2013, **34**, 558-565.
15. Y. Liu, J. Zhao, F. Li and Z. Chen, *J. Comput. Chem.*, 2013, **34**, 121-131.
16. N. Mardirossian and M. Head-Gordon, *J. Chem. Theory Comput.*, 2016, **12**, 4303-4325.
17. P. Mondal, P. K. Behera and N. K. Singha, *Chem. Commun.*, 2017, **53**, 8715.
18. P. Mondal, S. K. Raut and N. K. Singha, *J. Polym. Sci. A Polym. Chem.*, 2018, **56**, 2310.